Upper bound on the ergodic rate density of ALOHA wireless ad-hoc networks

Yaniv George, Itsik Bergel, *Senior Member, IEEE,* Ephraim Zehavi, *Fellow, IEEE*

Abstract

We present a novel upper bound on the Ergodic Rate Density (ERD) of ALOHA wireless ad-hoc networks. Our analysis uses a proper model of the physical layer together with an abstraction of higher communication layers. The novel bound is very general and supports various system models including for example, beamforming, spatial multiplexing, different fading models and different power control schemes. We also derive a closed form expression for the maximal gap between the novel bound and a known lower bound on the ERD. This expression is simple to evaluate and only depends on the path loss factor. For example, for a path loss factor of $\alpha = 3$ the novel upper bound is proved to be at most 31% higher than the lower bound (and hence also from the actual ERD). The usefulness and the generality of the novel bound is demonstrated by applications in multiple-antenna schemes. In particular, we study the optimization of the number of transmitted spatial streams in a MIMO network and derive the scaling of the ERD as the number of antennas grows. The results are further demonstrated using extensive simulations.

I. Introduction

Wireless Ad-hoc Networks (WANETs) offer simplicity and flexibility that make them suitable for many practical applications. These networks rely on decentralized channel access protocols (e.g., ALOHA [1] and Carrier Sense Multiple Access (CSMA) [2], [3]). Thus, WANETs can provide reliable communication without the need for any infrastructure.

In recent years, the analysis of random networks has generated considerable insights into the performance of WANETs. This type of analysis makes it possible to evaluate WANET performance without considering specific user locations. The most popular model for the positions of users in random WANETs is the homogeneous Poisson Point Process (PPP) [4]. In this model the number of users in each finite area has a Poisson distribution, and their locations are uniformly distributed over the area.

For the analysis of random WANETs, we follow the approach that uses exact modeling of the physical layer, together with a simplified abstraction of the other networking layers [4]–[7]. In this approach, performance is typically evaluated using network Area Spectral Efficiency (ASE), which is defined as the density of communicating pairs multiplied by their communication rates. The Transmission Capacity (TC) metric [8] is defined as the maximum achievable ASE given an outage constraint where all users use a fixed transmission rate. On the other hand, the Ergodic Rate Density (ERD) metric considers the communication rate of each pair as the mutual information between the transmitted signal and the received signal given the interferers' activity. The ERD is higher than the TC, but requires a somewhat more complicated transmission scheme, e.g., utilizing time diversity, frequency diversity, [9], or incremental-redundancy hybrid automatic repeat request (IR-HARQ), [10]–[12].

In this work we consider the ERD of ALOHA WANETs [9], [13]. The study of the ERD in WANETs has become somewhat simpler with the recent introduction of a general lower bound [7] which is applicable to any pre/post processing, fading distribution and power allocation scheme. The tightness of the bound was studied through simulations, and it was shown that the bound gives a good description of the behavior of the true ERD. However, [7] did not present an upper bound, and hence, the tightness of the bound was not evaluated analytically.

So far, the only upper bound on the ERD of ALOHA WANETs was presented by Stamatiou et al. [9] for the case where the nodes are equipped with multiple antennas and utilize a frequency hopping protocol. However, the model of Stamatiou et al. assumes constant transmission power and an absence of information in the receivers on the realization of the interfering channels. Both of these assumptions limit the applicability of the bound. The lack of channel state information (CSI) at the receivers characterizes specific networks. However, performance without receiver CSI is generally lower, [14], and the upper bound in Stamatiou et al. does not apply to more general networks. Moreover, the assumption of constant transmission power does not allow the study of power allocation schemes that may lead to higher performance.

In this work we generalize the bound presented in Stamatiou et al., and present a novel upper bound on the ERD of ALOHA WANETs that is applicable to the more general system model, presented in [7]. Thus, the novel bound is applicable to general power control schemes and general distributions of fading channels. Comparing the novel upper bound to the known lower bound of [7] enables us to present a closed form bound on the ratio between the lower bound

and the novel upper bound. This expression provides a simple evaluation of the tightness of the two bounds, and guarantees a maximum gap between the bounds. For example, for a path loss factor in the range of 2.5 to 4, the ratio between the bounds is shown to be at most in the range 18% to 47% respectively.

The generality of the upper bound is further used to obtain closed form expressions for the performance of WANETs utilizing Multiple-In-Multiple-Out (MIMO) antenna techniques.

So far, the performance of random MIMO WANETs have been studied mostly by the use of the TC performance metric (see for example [5] for various antenna diversity techniques). As stated above, in this work we focus on the ERD metric. In addition to its higher performance, the ERD metric also results in bounds that are simpler than the equivalent bounds on the TC. Furthermore, a typical TC framework includes an assumption of a small outage constraint [8], whereas the maximum spectral efficiency is typically achieved with large outage probabilities. The ERD upper bound presented here is valid for any user density and system parameters, and hence provides a simple and efficient tool for network optimizations. In the case of spatial multiplexing, the products of these optimizations are the optimum network density and the optimum number of streams.

Several works have investigated the tradeoff between spatial multiplexing and beamforming in MIMO WANETs. When the receivers perform interference cancellation of the undesired transmissions the optimum number of streams was shown to be one [6]. On the other hand, when the interference was considered as noise, spatial multiplexing was shown to have a potential gain [15]. In particular, increasing the number of streams was shown to be effective when the interference is limited (i.e., large path loss factor, large number of antennas or small density of users). The closed form expressions of the novel upper bound show that the insights in [15] are also valid for the ERD metric. Moreover, these expressions can be used to optimize the ERD for any active user density. We also show that the scaling gain of eigen-beamforming as a function of the number of transmit and receive antennas can be easily deduced from the bound for optimized density WANET and Rayleigh fading.

The rest of this paper is organized as follows: Section II describes the system model. Section III introduces the novel upper bound and an analytical evaluation of the tightness of the bound. Section IV introduces two applications of the novel upper bound for WANETs utilizing multiple antennas and Section V presents our concluding remarks.

A note on notation: For a matrix $\mathbf{A}$ the notation $\mathbf{A}^{\dagger}$ denotes the conjugate transpose and for a vector $\mathbf{v}$ the notation $\|\mathbf{v}\|^2 = \mathbf{v}^{\dagger}\mathbf{v}$ denotes its square Frobenius norm.

II. System Model

We assume a decentralized wireless ad-hoc network utilizing a slotted ALOHA protocol (e.g., [4]). Some of the nodes have data that need to be transmitted to specific destinations. Assuming the operation of a routing mechanism, each message is relayed to its destinations through multiple hops. For simplicity we assume that the receiver of the next hop for each message is located at a fixed distance, d, from the transmitter[1]. Nodes that have data to transmit can access the channel at any time slot with probability p. For any given time slot, the active transmitter distribution is modeled by a two dimensional PPP with a density of λ.

We assume that each node is equipped with N transmit antennas and M receive antennas. The channel matrix from transmitter j to the receiver i is denoted by $\mathbf{H}_{ij} \in (N \times M)$ with i.i.d. distributed entries. Each transmitter is assumed to perform spatial multiplexing of K streams [16] with $1 \leq K \leq \min(M, N)$.

The received signal at receiver i is given by:

$$\mathbf{r}_i = \sum_j \sqrt{\rho_j} X_{i,j}^{-\frac{\alpha}{2}} \mathbf{H}_{ij} \mathbf{z}_j + \mathbf{n}_i \tag{1}$$

where ρ_j is the transmission-power of the j-th transmitter, $X_{i,j}$ is the distance between the j-th transmitter and the i-th receiver respectively, $\mathbf{z}_j$ is the transmitted signal from transmitter j and $\mathbf{n}_i$ is the thermal noise. The path-loss factor is denoted by α (and the analysis is limited to $\alpha > 2$, which is required to bound the received energy). We assume that the network is operating at the interference limited regime, and therefore, in the remainder of the analysis we neglect the contribution of the thermal noise (setting $\mathbf{n}_i = 0$). Note that in this case normalizing the transmission power by a constant will not affect the final result.

We assume that the i-th transmitter has perfect channel knowledge of $\mathbf{H}_{ii}$, the channel matrix to the desired receiver, but no knowledge of any other channel matrix in the network. The Singular Value Decomposition (SVD) of the desired channel is given by $\mathbf{H}_{ii} = \mathbf{U}_i \mathbf{D}_i \mathbf{W}_i^{\dagger}$ where $\mathbf{U}_i$ and $\mathbf{W}_i$ are unitary matrices, and $\mathbf{D}_i = \mathrm{diag}\left([\gamma_{i,1}, ..., \gamma_{i,\min\{M,N\}}]\right)$ is a diagonal matrix with

[1]The bound can be trivially extended to any desired distribution of the distance to the desired transmitter.

the singular values of $\mathbf{H}_{ii}$ on its diagonal. Without loss of generality, we will assume throughout that the singular values are ordered so that $\gamma_{i,1} \geq \gamma_{i,2} \geq \ldots \geq \gamma_{i,\min\{M,N\}}$. The optimal precoding vector of the k-th stream at the i-th transmitter is given by the k-th column of $\mathbf{W}_i$, denoted by $\mathbf{w}_{i,k}$. The precoded signal of the i-th transmitter is therefore given by:

$$\mathbf{z}_i = \sum_{k=1}^{K} \mathbf{w}_{i,k} z_{i,k} \tag{2}$$

where $z_{i,k}$ denotes the data symbol of the k-th data stream for the i-th pair.

The receiver optimal decoding vector for the k-th stream is given by the k-th row of $\mathbf{U}_i^{\dagger}$, denoted by $\mathbf{u}_{i,k}^{\dagger}$, and hence the i-th receiver post-processed signal for the k-th stream is given by:

$$\widetilde{\mathbf{r}}_{i,k} = \mathbf{u}_{i,k}^{\dagger} \mathbf{r}_i. \tag{3}$$

Using the shift invariance property, [17], we analyze the performance of the network using a probe receiver. Without loss of generality, we assume that the probe receiver is located at the origin and for notational simplicity we drop the probe receiver index.

The k-th stream of the desired user is received at the probe receiver with a power of:

$$S_k = \rho_0 d^{-\alpha} \left\| \mathbf{u}_k^{\dagger} \mathbf{H}_0 \mathbf{W}_0 \right\|^2 = \rho_0 d^{-\alpha} \nu_k. \tag{4}$$

Without loss of generality we assume that $d = 1$.

The interference power contributed by transmitter j for the detection of the k-th spatial stream is given by:

$$\begin{aligned} T_{j,k} &= \left\| \sqrt{\rho_j} X_j^{-\frac{\alpha}{2}} \mathbf{u}_k^{\dagger} \mathbf{H}_j \mathbf{W}_j \right\|^2 \\ &= \rho_j X_j^{-\alpha} \eta_{j,k} \end{aligned} \tag{5}$$

where the second line used the definition $\eta_{j,k} \triangleq \left\| \mathbf{u}_k \mathbf{H}_j \mathbf{W}_j^{\dagger} \right\|^2$. As we assume that all channel matrices are statistically independent, the fading variables $\eta_{j,k}$ are statistically independent, and also statistically independent of all distance and transmission-power variables. Moreover, all fading variables that describe the k-th stream, $\eta_{j,k}$, have the same distribution.

The power of the aggregate interference, measured at the probe receiver in the k-th stream detector, is given by:

$$I_k = \sum_j T_{j,k} = \sum_j \rho_j X_j^{-\alpha} \eta_{j,k}. \tag{6}$$

The ergodic rate density (ERD) of the k-th spatial-stream of a network with an active user density of λ is given by [7]:

$$R_k(\lambda) = \lambda \cdot E\left[\log_2\left(1+\frac{S_k}{I_k}\right)\right] \tag{7}$$

In order to generalize our analysis we define the generic ERD:

$$\underline{R}_{f_V,f_Y,f_\rho}(\lambda) = \lambda \cdot E\left[\log_2\left(1+\frac{\rho_0 Y}{\sum_j \rho_j X_j^{-\alpha} V_j}\right)\right] \tag{8}$$

where we use the notations V and ρ when we only need an arbitrary representative of the corresponding Random Variable (R.V.) family. Thus, f_V and f_Y are the Probability Distribution Functions (PDFs) of the R.V.s V_j and Y respectively, and f_ρ is the PDF of the R.V.s ρ_0 and ρ_j.

Using the generic ERD definition of (8) we can now write the expression for the ERD of the probe pair, utilizing K spatial streams as:

$$R(\lambda) = \sum_{k=1}^{K} R_k(\lambda) = \sum_{k=1}^{K} \underline{R}_{f_\eta,f_{\nu_k},f_\rho}(\lambda). \tag{9}$$

Note that in the following we sometimes drop the subscript notations f_V, f_Y, f_ρ when the relevant distributions are easily understood from the context.

A useful lower bound on the ERD, which is helpful for the analysis herein, was originally presented in [7]. This lower bound on the ERD is given by:

$$\underline{R}_{f_V,f_Y,f_\rho}(\lambda) \geq R_{\mathrm{LB},f_V,f_Y,f_\rho}(\lambda) \tag{10}$$

where

$$R_{\mathrm{LB},f_V,f_Y,f_\rho}(\lambda) = \lambda e^{\frac{2}{\alpha}-1} \cdot E\left[\log_2\left(1+\frac{\rho \cdot Y}{C_\alpha \cdot \lambda^{\frac{\alpha}{2}}}\right)\right] \tag{11}$$

and

$$C_{\alpha,f_V,f_\rho} \triangleq \frac{2}{\alpha(\alpha-2)^{\frac{\alpha}{2}}}\left(\pi\alpha E\left[V^{\frac{2}{\alpha}}\right] E\left[\rho^{\frac{2}{\alpha}}\right]\right)^{\frac{\alpha}{2}}. \tag{12}$$

III. Performance Analysis

In the following section we present two theorems. The first theorem formulates a novel and general upper bound on the ERD. The second theorem provides information on the tightness of the bound, by bounding the ratio between the lower bound of [7] and the novel upper bound.

Theorem 1: An upper bound on the ERD of a network with an active user density of λ is:

$$\underline{R}_{f_V,f_Y,f_\rho}(\lambda) \leq R_{\text{UB},f_V,f_Y,f_\rho}(\lambda) \tag{13}$$

where

$$R_{\text{UB},f_V,f_Y,f_\rho}(\lambda) = \lambda \cdot E\left[\log_2\left(1+\frac{\rho \cdot Y}{\Lambda_\alpha \cdot \lambda^{\frac{\alpha}{2}}}\right)\right] \tag{14}$$

$$\Lambda_{\alpha,f_V,f_\rho} \triangleq \frac{\left(\pi E\left[V^{\frac{2}{\alpha}}\right] E\left[\rho^{\frac{2}{\alpha}}\right] \Gamma\left(1-\frac{2}{\alpha}\right)\right)^{\frac{\alpha}{2}}}{\Gamma\left(1+\frac{\alpha}{2}\right)}. \tag{15}$$

and $\Gamma(\cdot)$ represents the Gamma function.

Proof of Theorem 1: See Appendix A.

Similar to the lower bound in [7], the upper bound of Theorem 1 is very general, and can be used to support various schemes such as transmit and/or receive beamforming, threshold scheduling and inverse channel. These schemes can be supported by using the corresponding distributions of the fading variable (U, V) and power control variable (ρ) as was shown in [7].

Note that both the upper and lower bounds, (14) and (11), have a similar formulation. We next define:

$$\Omega_\alpha \triangleq C_{\alpha,f_V,f_\rho}^{-\frac{2}{\alpha}} \Lambda_{\alpha,f_V,f_\rho}^{\frac{2}{\alpha}} \tag{16}$$

and scale the density of the upper bound by Ω_α^{-1} compared to the density of the lower bound. Hence, the relation between the upper bound and the lower bound can be expressed by:

$$R_{\text{LB},f_V,f_Y,f_\rho}(\lambda) = e^{\frac{2}{\alpha}-1} \cdot \Omega_\alpha \cdot R_{\text{UB},f_V,f_Y,f_\rho}\left(\lambda \cdot \Omega_\alpha^{-1}\right). \tag{17}$$

Note that unlike C_{α,f_V,f_ρ} and $\Lambda_{\alpha,f_V,f_\rho}$, the relation parameter, Ω_α, is independent of the variables V and ρ and depends solely on the path loss factor. Using (12), (15) and the Gamma function property $Z \cdot \Gamma(Z) = \Gamma(1+Z)$ results in:

$$\begin{aligned}\Omega_\alpha &= \left(1-\frac{2}{\alpha}\right)\Gamma\left(1-\frac{2}{\alpha}\right)\left(\frac{2}{\alpha}\Gamma\left(1+\frac{\alpha}{2}\right)\right)^{-\frac{2}{\alpha}} \\ &= \Gamma\left(2-\frac{2}{\alpha}\right)\left(\Gamma\left(\frac{\alpha}{2}\right)\right)^{-\frac{2}{\alpha}}.\end{aligned} \tag{18}$$

In the following we will characterize the gap between the lower bound, (11), and the upper bound, (14). This gap characterization, given in Theorem 2, holds only up to the first local maximum of the upper bound. Thus, we need to properly define this local maximum.

We first note that the upper bound, (14), is a differentiable function of λ that satisfies $R_{\text{UB}}(\lambda) = 0$ both for $\lambda = 0$ and for $\lambda \to \infty$. It is also strictly positive for any $\lambda > 0$. Thus it has at least one local maximum. Define the active user density that achieves the first local maximum of the upper bound to be:

$$\lambda_{\star}^{\text{UB}} \triangleq \min\left\{\lambda : \frac{\partial R_{\text{UB}}(\lambda)}{\partial \lambda} = 0, \frac{\partial^2 R_{\text{UB}}(\lambda)}{\partial \lambda^2} < 0\right\}. \tag{19}$$

Recalling that $R_{\text{UB}}(0) = 0$ and $R_{\text{UB}}(\lambda) > 0$ for any $\lambda > 0$, there cannot be any local minimum of $R_{\text{UB}}(\lambda)$ in the range $0 < \lambda < \lambda_{\star}^{\text{UB}}$. The lower bound function exhibits the same behavior, and we also define:

$$\lambda_{\star}^{\text{LB}} \triangleq \min\left\{\lambda : \frac{\partial R_{\text{LB}}(\lambda)}{\partial \lambda} = 0, \frac{\partial^2 R_{\text{LB}}(\lambda)}{\partial \lambda^2} < 0\right\}. \tag{20}$$

Using (17) leads to the simple relation:

$$\lambda_{\star}^{\text{LB}} = \Omega_{\alpha} \cdot \lambda_{\star}^{\text{UB}}. \tag{21}$$

In most practical networks the upper and lower bounds have a single extremum, and hence, $\lambda_{\star}^{\text{UB}}$ and $\lambda_{\star}^{\text{LB}}$ represent the global optimum of these functions. For example, in the case of fixed transmission power and no fading (i.e., $Y = 1$) the location of the global maxima of the upper and lower bounds are given by [18]:

$$\begin{aligned}\lambda_{\star}^{\text{UB}} &= \left(\Lambda_{\alpha}\left(e^{\Xi_{\alpha}} - 1\right)\right)^{-\frac{2}{\alpha}} \\ \lambda_{\star}^{\text{LB}} &= \left(C_{\alpha}\left(e^{\Xi_{\alpha}} - 1\right)\right)^{-\frac{2}{\alpha}}\end{aligned} \tag{22}$$

respectively, where

$$\Xi_{\alpha} \triangleq \frac{\alpha}{2} + W\left(-\frac{\alpha}{2}e^{-\frac{\alpha}{2}}\right) \tag{23}$$

and $W(\cdot)$ is the product-log function also known as the Lambert W function. It is easy to verify that the curves of the bounds for other common distributions (such as Rayleigh and Rician fading) also have a single extremum point[2]. However, for generality, in the following we characterize the bound tightness in terms of its first local maximum.

From a network point of view, the first local maximum represents the highest density for practical use [19]. Above this density, the network may experience instability, because any small

[2]Bounds on the ratio of two functions with a similar formation were presented in [14] for the specific case of Rayleigh fading without the assumption of a single extremum.

increase in the number of transmissions will cause the network throughput to decrease and require additional retransmissions. Thus, we characterize the network for $\lambda \leq \lambda_{\star}^{\mathrm{LB}}$.

Theorem 2: For an active user density of $\lambda \leq \lambda_{\star}^{\mathrm{LB}}$, the ratio between the upper bound and the ERD is bounded by:

$$\frac{\underline{R}_{f_V,f_Y,f_\rho}(\lambda)}{R_{\mathrm{UB},f_V,f_Y,f_\rho}(\lambda)} \geq \frac{R_{\mathrm{LB},f_V,f_Y,f_\rho}(\lambda)}{R_{\mathrm{UB},f_V,f_Y,f_\rho}(\lambda)} \geq e^{\frac{2}{\alpha}-1} \cdot \Omega_\alpha \tag{24}$$

where Ω_α is defined in (18).

Proof of Theorem 2: See Appendix B.

To demonstrate the tightness of the upper and lower bounds we present a comparison of the derived analytical expressions and the actual ERD which is evaluated through simulations. The ERD in the simulations was evaluated using a Monte-Carlo network simulator averaging 10^5 network realizations. The channels between each transmit and receive antenna are distributed as Rayleigh fading.

Fig. 1 depicts the upper bound, (14), the ERD, (8), and the lower bound, (11), as a function of the active user density, for single antennas, fixed transmission power and a path loss factor of $\alpha = 3$. As shown in the figure, both the novel upper bound and the lower bound give a good characterization of the ERD (and for large user densities, the curve of the upper bound merges with the curve of the ERD). As was noted above, the curves of the ERD and the bounds as a function of user density have a single extremum point.

Fig. 2 depicts the maximum rate density for the upper bound, the ERD and the lower bound as a function of α for single antennas and a fixed transmission power policy. The maximum ERDs of the upper and lower bounds are given by $R_{\mathrm{UB}}\left(\lambda_{\star}^{\mathrm{UB}}\right)$ and $R_{\mathrm{LB}}\left(\lambda_{\star}^{\mathrm{LB}}\right)$ respectively and the maximum ERD is given by $\max_\lambda R(\lambda)$. As can be seen, the upper bound is especially tight for small values of the path loss factor. The ratio between the upper bound and the ERD decreases with α and is approximately equal to 0.97 and 0.73 for path loss factors of 2.5 and 4 respectively. These ratios are better observed in Fig. 3 which depicts the ratios for the curves in Fig. 2 in addition to the expression of the minimum ratio between the bounds (24). The upper curve depicts the ratio between the ERD and the upper bound and the curve below it depicts the ratio between the lower bound and the ERD. The two lower curves depict the ratio between the upper and lower bounds and the analytic bound on this ratio (24). As can be observed, all curves decrease with α and the actual ratio between the bounds is very close to its minimum

(24). For the interesting area in which the path loss factor is within the range of $2.5 \leq \alpha \leq 4$ equation (24) indicates that the gap between the bounds is at most 18% to 47% (and exactly 31% for $\alpha = 3$). Although for larger α the two bounds become further apart, the closed form expression (24) is still informative since it gives a simple guarantee on the usefulness of the two bounds.

IV. Applications of the bound

In this section we present two applications of the upper bound utilizing multiple-antenna techniques. We assume a rich scattering environment which results in a Rayleigh fading channel between each transmit and receive antenna in the network. The channels are assumed to be normalized and the channel matrix $\mathbf{H}$ distributes as a central complex Wishart matrix [16], [20] with $\mathcal{CN}(0,1)$ entries[3].

A. Single Stream Beamforming

We next analyze the case of transmit beamforming with N transmit antennas and a single receive antenna, i.e., $M = 1$. We also assume the use of a simple channel inversion power control strategy (i.e., $\rho(Y) = Y^{-1}$).

The preprocessing of beamforming over N antennas results in a Chi-square desired channel distribution, with $2N$ degrees of freedom, $2Y \sim \chi^2_{2N}$, which leads to:

$$E\left[\rho^{\frac{2}{\alpha}}(Y)\right] = E\left[Y^{-\frac{2}{\alpha}}\right] = \frac{\Gamma\left(N - \frac{2}{\alpha}\right)}{\Gamma(N)}. \tag{25}$$

This preprocessing does not change the interference channel statistics, V. In this case $V = \eta_k$ has a Chi-square distribution and hence, the expectation over V in (15) is:

$$E\left[V^{\frac{2}{\alpha}}\right] = \Gamma\left(1 + \frac{2}{\alpha}\right). \tag{26}$$

Substituting (26) and (25) into Theorem 1 leads to:

$$R^{\mathrm{B}}_{\mathrm{UB}}(\lambda) = \lambda \cdot \log_2\left(1 + \frac{1}{\Lambda^{\mathrm{B}}_{\alpha} \cdot \lambda^{\frac{\alpha}{2}}}\right) \tag{27}$$

[3]Recall that we assume to be working in the interference limited regime. Hence, the average transmission power has no impact on network performance.

where B stands for beamforming and

$$\Lambda_{\alpha}^{\mathrm{B}} \triangleq \frac{\left(\pi\Gamma\left(N-\frac{2}{\alpha}\right)\Gamma\left(1-\frac{2}{\alpha}\right)\Gamma\left(1+\frac{2}{\alpha}\right)\right)^{\frac{\alpha}{2}}}{\Gamma\left(1+\frac{\alpha}{2}\right)\left(\Gamma(N)\right)^{\frac{\alpha}{2}}}. \tag{28}$$

This upper bound has the same form as the lower bound on the ERD for the case of transmit beamforming in [7], except for parameter $\Lambda_{\alpha}^{\mathrm{B}}$. Thus, the closed form expression for optimal user density can be easily adapted from the results in [7], and is given by:

$$\lambda_{\star}^{\mathrm{B}} = \arg\max_{\lambda} R_{\mathrm{UB}}^{\mathrm{B}}(\lambda) = \left(\Lambda_{\alpha}^{\mathrm{B}}\left(e^{\Xi_{\alpha}}-1\right)\right)^{-\frac{2}{\alpha}} \tag{29}$$

where Ξ_{α} is defined in (23). The optimum upper bound can be written as:

$$R_{\mathrm{UB}}^{\mathrm{B}}\left(\lambda_{\star}^{\mathrm{B}}\right) = \frac{\lambda_{\star}^{\mathrm{B}} \cdot \Xi_{\alpha}}{\ln(2)}. \tag{30}$$

The ergodic rate density for the case of transmitter beamforming and channel inversion power control with various number of antennas is illustrated in Fig. 4. The figure depicts the upper bound, (27), the ERD, and the lower bound, [7, eq. 30] as a function of the active user density for $M = 1$, $N = 1, 3, 9$ antennas, and a path loss factor of $\alpha = 3$. The analytical maximum rate density of the upper bound (30) is 0.06, 0.27 and 0.65 whereas the measured maximum ERD is 0.053, 0.24 and 0.57 for $N = 1, 3, 9$ respectively. In all three cases the ERD is at most 13% below the upper bound which indicates the tightness of the upper bound and its usefulness for optimal ERD evaluation.

B. Spatial Multiplexing

In this subsection we analyze the performance of WANETs that utilize spatial multiplexing. We assume that each pair is equipped with an equal number of transmit and receive antennas; i.e., $N = M$ and that each pair delivers its information using a constant number of spatial streams, denoted by K, where $1 \leq K \leq M$. We further assume that each pair delivers its data over the first (largest) K singular values.

For a transmission of K spatial streams the interference power contributed by each interferer is distributed as a Chi-square with $2K$ degrees of freedom and a mean of K; i.e., $2V \sim \chi_{2K}^2$, which results in:

$$E\left[(\eta_k)^{\frac{2}{\alpha}}\right] = E\left[V^{\frac{2}{\alpha}}\right] = \frac{\Gamma\left(K+\frac{2}{\alpha}\right)}{\Gamma(K)}. \tag{31}$$

Substituting (8) and (31) into (9) and using Theorem 1 results in the following upper bound for the spatial multiplexing case,

$$R_{\mathrm{UB}}^{\mathrm{S}}\left(\lambda,K\right)=\lambda\cdot\sum_{k=1}^{K}E\left[\log_2\left(1+\frac{\nu_k}{\Lambda_\alpha^{\mathrm{S},K}\cdot\lambda^{\frac{\alpha}{2}}}\right)\right] \tag{32}$$

where S stands for spatial multiplexing, and

$$\Lambda_\alpha^{\mathrm{S},K}\triangleq\frac{\left(\pi\Gamma\left(K+\frac{2}{\alpha}\right)\Gamma\left(1-\frac{2}{\alpha}\right)\right)^{\frac{\alpha}{2}}}{\Gamma\left(1+\frac{\alpha}{2}\right)\left(\Gamma\left(K\right)\right)^{\frac{\alpha}{2}}}. \tag{33}$$

Note that (33) can be further simplified by using Kershaw's inequality, [21], [22]:

$$\frac{\Gamma\left(K+\frac{2}{\alpha}\right)}{\Gamma\left(K\right)}\geq\left(K-\frac{1}{2}+\frac{1}{\alpha}\right)^{\frac{2}{\alpha}} \tag{34}$$

which is very tight for all values of $\alpha>2$ and $K\geq1$.

The number of streams, K, affects the upper bound in three different ways in (34). The sum outside the expectation increases the ERD as the number of streams increases. The second effect is on the distribution of the k-th stream power, which is obviously less preferable than the power of previous streams (due to the assumption that the singular values are ordered in decreasing order). Thus, the expected rate of the k-th stream is lower than the rate of previous streams. These two effects are similar in nature to the behavior of MIMO in the single user scenario. But in the WANET case, there is also a third effect, through the effect of the number of streams on the interference. This effect is seen through the $\Lambda_\alpha^{\mathrm{S},K}$ term in the denominator of (32) as K increases (considering (34), for large K, $\Lambda_\alpha^{\mathrm{S},K}$ is approximately linear with K). This increase in the interference term has a negative impact on all streams (and not only on the last stream added). Thus, the use of a large number of spatial streams is less favorable than in the case of single user MIMO, even if the transmission power is high. Hence, finding the optimal number of streams in (32) is not trivial.

It is also interesting to compare the increase in the number of spatial streams per user to the increase in the user density by the same ratio in (32). In both approaches the overall number of streams in the network remain constant. However increasing K will approximately increase the interference linearly with K whereas increasing the active user density will increase the interference by a factor of $\lambda^{\frac{\alpha}{2}}$. This can be explained by two differences between the two approaches. The first difference is that the receiver achieves complete interference cancellation between the streams of the desired user. Thus, increasing K has a smaller effect on the received

interference than the equivalent increase in the number of nodes. Furthermore, increasing the node density also increases the probability of having a nearby interferer whereas increasing the number of streams only affects the distribution of the power contributed by each interferer. Thus, in terms of interference, it is always more beneficial to increase K than to increase the node density by the same ratio.

On the other hand, if the interference term, $\Lambda_{\alpha}^{\mathrm{S},K} \cdot \lambda^{\frac{\alpha}{2}}$, is very large, the upper bound (32) can be approximated by:

$$R_{\mathrm{UB}}^{\mathrm{S}}\left(\lambda, K\right) \simeq \frac{\lambda^{1-\frac{\alpha}{2}} \Gamma\left(1+\frac{\alpha}{2}\right)}{\left(\pi \Gamma\left(1-\frac{2}{\alpha}\right)\right)^{\frac{\alpha}{2}} \ln(2)} \cdot \frac{1}{K-\frac{1}{2}+\frac{1}{\alpha}} \sum_{k=1}^{K} E[\nu_k] \tag{35}$$

where we used $\log\left(1+x\right) \simeq x$ and (34). Recalling that $\alpha > 2$, the expression in (35) is clearly optimized by the eigen-beamforming scheme; i.e., $K = 1$.

Optimizing the network parameters of (32) requires a two dimensional optimization. This optimization can be performed in two steps. The first step optimizes the density of active users for each number of streams, K, i.e.:

$$R_{\mathrm{UB}}^{\mathrm{S}}\left(\lambda_{\star}^{\mathrm{S},K}, K\right) = \max_{\lambda} R_{\mathrm{UB}}^{\mathrm{S}}(\lambda, K), \;\; K \in \{1, 2, \ldots, M\}\,. \tag{36}$$

The second step optimizes the number of streams:

$$R_{\mathrm{UB}}^{\mathrm{S}}\left(\lambda_{\star}^{\mathrm{S}}, K_{\star}^{\mathrm{S}}\right) = \max_{K \in \{1,2,\ldots,M\}} R_{\mathrm{UB}}^{\mathrm{S}}\left(\lambda_{\star}^{\mathrm{S},K}, K\right). \tag{37}$$

Fig. 5 depicts the upper bound (32) as a function of the active user density for $N = M = 6$, $\alpha = 4$, Rayleigh fading channels, and $K = 1, 2, 3, 4, 5, 6$. The figure shows that for a low density of active users ($\lambda < 0.03$) the optimal number of streams is equal to the maximum available; i.e., $K = 6$. When the density of nodes grows, the optimal number of streams decreases and for a high density of active users ($\lambda > 0.75$) eigen-beamforming ($K = 1$) is the optimal selection. Note also that the ERD has a single maximum for each selection of K. Further insights on the curves' maxima can be derived from Fig. 6.

Fig. 6 depicts the maximum rate density of the upper bound (presented in (36)), the ERD and the rate density of the lower bound (integration of (11) and (9)) as a function of the optimal active user density for $N = M = 6$, and $\alpha = 4$. The figure only shows the point that represents the maximum of each curve, for $K = 1, 2, 3, 4, 5, 6$. For each K the location of the point is determined according to the maximum ERD achieved by this number of streams (y-axis) and

the active user density that achieves this maximum (x-axis). Note that the optimal user density, $\lambda_\star^{\mathrm{S},K}$, is a decreasing function of the number of spatial streams, K.

As can be seen, the curve of both bounds exhibits the same behavior as the actual ERD. But the upper bound gives better predictions for the optimal user density for any given number of streams. In addition, all curves are maximized for $K_\star^{\mathrm{S}} = 3$. Thus, the optimum active user density (defined by (37)) is $\lambda_\star^{\mathrm{S}} = 0.25$, the maximal upper bound on the ERD is $R_{\mathrm{UB}}^{\mathrm{S}}\left(\lambda_\star^{\mathrm{S}}, K_\star^{\mathrm{S}}\right) = 1.66$ bit/sec/m^2 and the maximal ERD is 1.22 bit/sec/m^2. Note that the ratio between the maximum of the lower bound and the maximum of the upper bound is exactly 54% as was anticipated by Theorem 2.

Unlike the case of single user MIMO, the additional gain from spatial multiplexing in density-optimized WANETs seems to be quite limited compared to the eigen-beamforming scheme ($K = 1$). Capacity analysis in single user MIMO shows that the spectral efficiency increases monotonically with the number of spatial streams, and that the capacity gain approaches M for high enough SNR. In contrast, in the WANET MIMO case, the ERD is not monotonic with the number of spatial streams. In the example in Fig. 6, plotted for the high SNR regime and density-optimized WANETs, the gain from the selection of the optimal number of streams compared to the eigen-beamforming scheme is only 20%. It is important to emphasize that the limited gain of spatial multiplexing does not mean that the gain of multiple antennas is limited. Rather, it shows that in a density optimized WANET, even a single stream WANET gains significantly from the use of multiple antennas.

The upper bound can also be used to analyze the asymptotic behavior of MIMO WANETs as the number of antennas grows, i.e., $M \to \infty$. We first analyze the density optimized eigen-beamforming case. For Rayleigh fading, the normalized largest singular value converges to $\lim_{M\to\infty} \nu_1/_M = 4M$, [23]. Substituting into (32) and using the change of variables $\lambda' = \lambda M^{-\frac{2}{\alpha}}$ results in

$$\lim_{M\to\infty} \frac{R_{\mathrm{UB}}^{\mathrm{S}}\left(\lambda', 1\right)}{M^{\frac{2}{\alpha}}} = \lambda' \cdot E\left[\log_2\left(1 + \frac{4}{\Lambda_\alpha^{\mathrm{S},1} \cdot \left(\lambda'\right)^{\frac{\alpha}{2}}}\right)\right]. \tag{38}$$

Thus, the density optimized ERD can be approximated as

$$R_{\mathrm{UB}}^{\mathrm{S}}\left(\lambda_\star^{\mathrm{S}}, 1\right) \simeq M^{\frac{2}{\alpha}} \cdot \max_{\lambda'} \lambda' \cdot E\left[\log_2\left(1 + \frac{4}{\Lambda_\alpha^{\mathrm{S},1} \cdot \left(\lambda'\right)^{\frac{\alpha}{2}}}\right)\right], \tag{39}$$

and the ERD of density optimized WANET that transmits a single stream scales as $M^{\frac{2}{\alpha}}$. This matches the TC scaling derived for the case of eigen-beamforming in [5]. Note that [24] showed a linear scaling of the SIR with the number of antennas. This linear scaling can be translated into linear scaling of the ERD, but only under a strong interference assumption. This assumption does not hold when the number of antennas is very large, and hence the actual scaling of the ERD is only as $M^{\frac{2}{\alpha}}$.

In order to analyze the case of multiple stream transmission we allow K to increase with M, but keep the ratio between the number of streams and the number of antennas as constant, denoted by $\beta \triangleq {}^{K}/_{M}$. Define the empirical Cumulative Density Function (CDF) of the normalized stream power, $F_{\frac{\nu}{M}}(x) = \dfrac{1}{M}\sum_{i=k}^{\infty} \mathbf{1}\left(\dfrac{\nu_i}{M} < x\right)$ where $\mathbf{1}$(condition) is the indicator function which equals 1 if the condition is satisfied and zero otherwise. For an asymptotic number of antennas and Rayleigh fading, the empirical CDF converges, and the corresponding PDF is given by [25]:

$$\lim_{M\to\infty} f_{\frac{\nu}{M}}(x) = \frac{1}{2\pi}\sqrt{\frac{4-x}{x}} \tag{40}$$

where $0 < x < 4$. Defining $\psi(\beta) \triangleq \lim\limits_{M\to\infty} \dfrac{\nu_K}{M}$ leads to the relation:

$$\frac{1}{2\pi}\int_{\psi(\beta)}^{4} \sqrt{\frac{4-x}{x}}dx = \beta. \tag{41}$$

Thus, for an asymptotic number of antennas the summation in the upper bound, (32), converges to:

$$\begin{aligned}\lim_{M\to\infty} \frac{R_{\text{UB}}^{\text{S}}}{M}(\lambda, K) &= \lim_{M\to\infty} \frac{\lambda}{M}\int_{\psi(\beta)}^{4} \log_2\left(1 + \frac{M\cdot x}{\Lambda_{\alpha}^{\text{S},K}\cdot\lambda^{\frac{\alpha}{2}}}\right) \\ &\quad \cdot\left(M\cdot f_{\frac{\nu}{M}}(x)\right)dx \\ &= \frac{\lambda}{2\pi}\int_{\psi(\beta)}^{4} \log_2\left(1 + \frac{x}{L_\alpha\lambda^{\frac{\alpha}{2}}}\right) \\ &\quad \cdot\sqrt{\frac{4-x}{x}}dx \end{aligned} \tag{42}$$

where the second line substituted (40) and the definition:

$$L_\alpha \triangleq \lim_{M\to\infty} \frac{M}{\Lambda_{\alpha}^{\text{S},K}}. \tag{43}$$

Using (34) we have $L_\alpha = \dfrac{\Gamma\left(1+\frac{\alpha}{2}\right)\cdot\beta}{\left(\pi\Gamma\left(1-\frac{2}{\alpha}\right)\right)^{\frac{\alpha}{2}}}$. One can readily verify that the integral in the last line of (42) exists and is bounded for any $\alpha > 2$. Hence, the scaling law of the ERD for spatial

multiplexing WANET is linear with the number of antennas, M, for any value of λ and β. As the lower bound of (11) has the same structure as the analyzed upper bound, it also results in the same scaling of the ERD with the number of antennas. Thus, the linear scaling that was proved in (42) is the exact scaling of the ERD (and not only an upper bound).

The linear scaling of the ERD with the number of antennas is similar to the known scaling of TC in MIMO WANETs [6], [26]. However, the linear TC scaling was derived for WANETs that employed interference cancellation of neighboring transmissions, while our result only requires spatial multiplexing. This difference is important, because cancellation of neighboring transmission requires channel measurements of many neighbor transmissions, which is not needed for spatial multiplexing.

To conclude the MIMO WANET example, we summarize as follows: when the number of spatial streams decreases, the optimal density of active users increases. For a small path loss factor (which results in high interference) eigen-beamforming is likely to be the optimal scheme; for a general path loss factor, a two-dimensional optimization of both the density of active users and the number of streams is essential to achieve the maximum ERD. Nevertheless, the gain from the optimal spatial-multiplexing scheme compared to eigen-beamforming in density-optimized WANETs is much smaller than the potential capacity gain of single user MIMO. For large number of antennas, M, the ERD scales as $M^{\frac{2}{\alpha}}$ for eigen-beamforming, and as M when the number of spatial streams is optimized.

V. Conclusion

We derived a novel upper bound on the ergodic rate density of random WANETs. The upper bound is very general and can support various transmission/reception schemes and general fading distributions.

The formula of the upper bound is shown to be similar to the formula of a recently published lower bound. This similarity is utilized for the quantification of the maximum gap between the bounds. The maximum gap was presented as a closed form expression which bounds the ratio between the two bounds and is only a function of the path loss factor. This expression shows that for all cases of practical interest, the ratio between the bounds is at most 50% (for example, for a path loss factor of 3 the gap between the bounds is shown to be at most 31%).

The usefulness and the simplicity of the bound was demonstrated by two applications: beamforming and spatial multiplexing. For the beamforming application we presented analytical expressions for the optimal density of active users and the optimal ERD as a function of the number of antennas. For the application of spatial-multiplexing we presented an upper bound that depends on the number of antennas, the number of spatial streams and the density of active users. We also proved that for large number of antennas, M, the ERD scales as $M^{\frac{2}{\alpha}}$ for eigen-beamforming, and as M when the number of spatial streams is optimized.

APPENDIX A
PROOF OF THEOREM 1

Substituting (4) into (8) and using Jensen's inequality results in:

$$\underline{R}_{f_V,f_Y,f_\rho}(\lambda)) \leq \lambda \cdot E\left[\log_2\left(1+E\left[\frac{1}{I}\right]\cdot\rho\cdot Y\right)\right]. \tag{44}$$

Denote the Probability Density Function (PDF) of the interference, I, by $f_I(I)$. Motivated by the mathematical formulation in [9, proof of proposition 2], we use the relation between the characteristic function of I and the expectation of its inverse:

$$\begin{aligned} E\left[\frac{1}{I}\right] &= \int_0^\infty \left(\frac{1}{I}\right) f_I(I)\, dI \\ &= \int_0^\infty \left(\int_0^\infty e^{-sI} ds\right) f_I(I)\, dI \\ &= \int_0^\infty \left(\int_0^\infty f_I(I)\, e^{-sI} dI\right) ds \\ &= \int_0^\infty E\left[e^{-sI}\right] ds \\ &= \int_0^\infty \Phi(s) ds \end{aligned} \tag{45}$$

where $\Phi(s) = E\left[e^{-sI}\right]$ is the characteristic function of I. The PDF of the interference, $f_I(I)$, has no known closed-form expression. However, its characteristic function is known and given by (e.g., [27], [28]):

$$\begin{aligned} \Phi(s) &= \exp\left(-\lambda \int_0^\infty E\left[1-e^{-sV\rho r^{-\alpha}}\right] 2\pi r dr\right) \\ &= \exp\left(-\pi\lambda s^{\frac{2}{\alpha}} E\left[V^{\frac{2}{\alpha}}\right] E\left[\rho^{\frac{2}{\alpha}}\right] \Gamma\left(1-\frac{2}{\alpha}\right)\right). \end{aligned} \tag{46}$$

Substituting (46) into (45) results in:

$$\begin{aligned} E\left[\frac{1}{I}\right] &= \int_0^\infty e^{-\pi\lambda E\left[V^{\frac{2}{\alpha}}\right]E\left[\rho^{\frac{2}{\alpha}}\right]\Gamma\left(1-\frac{2}{\alpha}\right)x^{\frac{2}{\alpha}}}dx \\ &= \Gamma\left(1+\frac{\alpha}{2}\right)\left(\pi\lambda E\left[V^{\frac{2}{\alpha}}\right]E\left[\rho^{\frac{2}{\alpha}}\right]\Gamma\left(1-\frac{2}{\alpha}\right)\right)^{-\frac{\alpha}{2}} \\ &= \frac{1}{\Lambda_\alpha \lambda^{\frac{\alpha}{2}}} \end{aligned} \tag{47}$$

where Λ_α is defined in (15). Substituting (47) into (44) concludes the proof. □

APPENDIX B
PROOF OF THEOREM 2

The left-hand side of the inequality in (24) is trivial from the definition of the lower bound. The theorem considers the density range of:

$$\lambda \leq \lambda_\star^{\text{LB}} = \lambda_\star^{\text{UB}} \cdot \Omega_\alpha \tag{48}$$

where (21) was used. For $\lambda \leq \lambda_\star^{\text{UB}}$ the upper bound, $R_{\text{UB},f_V,f_Y,f_\rho}(\lambda)$, increases with λ. Thus, using $\Omega_\alpha \leq 1$ (which is proved by Lemma 1 below) leads to:

$$R_{\text{UB},f_V,f_Y,f_\rho}\left(\lambda \cdot \Omega_\alpha^{-1}\right) \geq R_{\text{UB},f_V,f_Y,f_\rho}(\lambda) \;\; \forall \lambda \leq \lambda_\star^{\text{LB}}. \tag{49}$$

Substituting (49) into (17) proves the right-hand side of the inequality in (24) and concludes the proof of the theorem. □

Lemma 1: For any $\alpha > 2$, the value of Ω_α, defined in (18), satisfies: $\Omega_\alpha \leq 1$.

Proof of Lemma 1: Starting from the inequality [29]:

$$\frac{\left(\Gamma(x+1)\right)^a}{\Gamma(ax+1)} \leq 1 \;,\; \forall x \in [0,1],\; a \geq 1 \tag{50}$$

and substituting $x = 1 - \frac{2}{\alpha}$ and $a = \frac{\alpha}{2}$ leads to:

$$\frac{\left(\Gamma\left(2-\frac{2}{\alpha}\right)\right)^{\frac{\alpha}{2}}}{\Gamma\left(\frac{\alpha}{2}\right)} \leq 1. \tag{51}$$

Raising both sides of (51) to the power of $2/\alpha$ and using Definition (18) concludes the proof of the lemma. ■

REFERENCES

[1] N. Abramson, "The ALOHA system - another alternative for computer communications," in *AFIPS computer conference*, 1970, pp. 281–285.

[2] L. Kleinrock and F. Tobagi, "Packet switching in radio channels: Part I–carrier sense multiple-access modes and their throughput-delay characteristics," *IEEE Transactions on Communications*, vol. 23, no. 12, pp. 1400–1416, 1975.

[3] Y. George and I. Bergel, "The spectral efficiency of slotted CSMA ad-hoc networks with directional antennas," *IEEE Transactions on Wireless Communications*, vol. 11, no. 10, pp. 3799 –3809, 2012.

[4] F. Baccelli, B. Blaszczyszyn, and P. Muhlethaler, "An ALOHA protocol for multihop mobile wireless networks," *IEEE Transactions on Information Theory*, vol. 52, no. 2, pp. 421–436, 2006.

[5] A. Hunter, J. Andrews, and S. Weber, "Transmission capacity of ad hoc networks with spatial diversity," *IEEE Transactions on Wireless Communications*, vol. 7, pp. 5058–5071, 2008.

[6] R. Vaze and R.W. Heath, "Transmission capacity of ad-hoc networks with multiple antennas using transmit stream adaptation and interference cancellation," *IEEE Transactions on Information Theory*, vol. 58, no. 2, pp. 780–792, 2012.

[7] Y. George, I. Bergel, and E. Zehavi, "The ergodic rate density of aloha wireless ad-hoc networks," *IEEE Transactions on Wireless Communications*, vol. 12, no. 12, pp. 6340–6351, 2013.

[8] S. Weber, J.G. Andrews, and N. Jindal, "An overview of the transmission capacity of wireless networks," *IEEE Transactions on Communications*, vol. 58, no. 12, pp. 3593–3604, 2010.

[9] K. Stamatiou, J.G. Proakis, and J.R. Zeidler, "Channel diversity in random wireless networks," *IEEE Transactions on Wireless Communications*, vol. 9, no. 7, pp. 2280–2289, 2010.

[10] D. Mandelbaum, "An adaptive-feedback coding scheme using incremental redundancy," *IEEE Transactions on Information Theory*, vol. 20, no. 3, pp. 388–389, 1974.

[11] R. Comroe and D. Costello Jr, "ARQ schemes for data transmission in mobile radio systems," *IEEE Journal on Selected Areas in Communications*, vol. 2, no. 4, pp. 472–481, 1984.

[12] G. Caire and D. Tuninetti, "The throughput of hybrid-ARQ protocols for the gaussian collision channel," *IEEE Transactions on Information Theory*, vol. 47, no. 5, pp. 1971–1988, 2001.

[13] M. Haenggi, "Outage, local throughput, and capacity of random wireless networks," *IEEE Transactions on Wireless Communications*, vol. 8, no. 8, pp. 4350–4359, 2009.

[14] Y. George, I. Bergel, and E. Zehavi, "The effect of imperfect CSI on the performance of random ad-hoc networks," *To be published in Proceedings of the International Conference on Communications (ICC)*, 2014.

[15] A.M. Hunter and J.G. Andrews, "Adaptive rate control over multiple spatial channels in ad hoc networks," in *Modeling and Optimization in Mobile, Ad Hoc, and Wireless Networks and Workshops (WiOPT)*, 2008, pp. 469–474.

[16] E. Telatar, "Capacity of multi-antenna gaussian channels," *European transactions on telecommunications*, vol. 10, no. 6, pp. 585–595, 1999.

[17] D. Stoyan, W.S. Kendall, and J. Mecke, *Stochastic Geometry and Its Applications*, John Wiley & Sons Inc., 1995.

[18] Y. George, I. Bergel, and E. Zehavi, "Novel lower bound on the ergodic rate density of random ad-hoc networks," in *Proceedings of IEEE Signal Processing Advances in Wireless Communications (SPAWC)*, 2013, pp. 580–584.

[19] J.H. Sarker and S.J. Halme, "An optimum retransmission cut-off scheme for slotted ALOHA," *Wireless Personal Communications*, vol. 13, pp. 185–202, 2000.

[20] A.T. James, "Distributions of matrix variates and latent roots derived from normal samples," *The Annals of Mathematical Statistics*, vol. 35, no. 2, pp. 475–501.

[21] D. Kershaw, "Some extensions of W. Gautschi's inequalities for the Gamma function," *Mathematics of Computation*, vol. 41, no. 164, pp. 607–611, 1983.

[22] F. Qi and L. Losonczi, "Bounds for the ratio of two Gamma functions," *Journal of Inequalities and Applications*, p. 204, 2010.

[23] I.M Johnstone, "On the distribution of the largest eigenvalue in principal components analysis," *Annals of statistics*, pp. 295–327, 2001.

[24] B. Chen and M.J. Gans, "MIMO communications in ad hoc networks," *IEEE Transactions on Signal Processing*, vol. 54, no. 7, pp. 2773–2783, 2006.

[25] D. Jonsson, "Some limit theorems for the eigenvalues of a sample covariance matrix," *Journal of Multivariate Analysis*, vol. 12, no. 1, pp. 1–38, 1982.

[26] N. Jindal, J.G. Andrews, and S. Weber, "Rethinking MIMO for wireless networks: Linear throughput increases with multiple receive antennas," in *IEEE International Conference on Communications (ICC)*, 2009, pp. 1–6.

[27] J. Venkataraman, M. Haenggi, and O. Collins, "Shot noise models for outage and throughput analyses in wireless ad hoc networks," pp. 1–7, 2006.

[28] SB Lowen and MC Teich, "Power-law shot noise," *IEEE Transactions on Information Theory*, vol. 36, pp. 1302–1318, 1990.

[29] J. Sandor, "A note on certain inequalities for the gamma function," *Journal of Inequalities in Pure and Applied Mathematics*, vol. 6, no. 3, 2005.

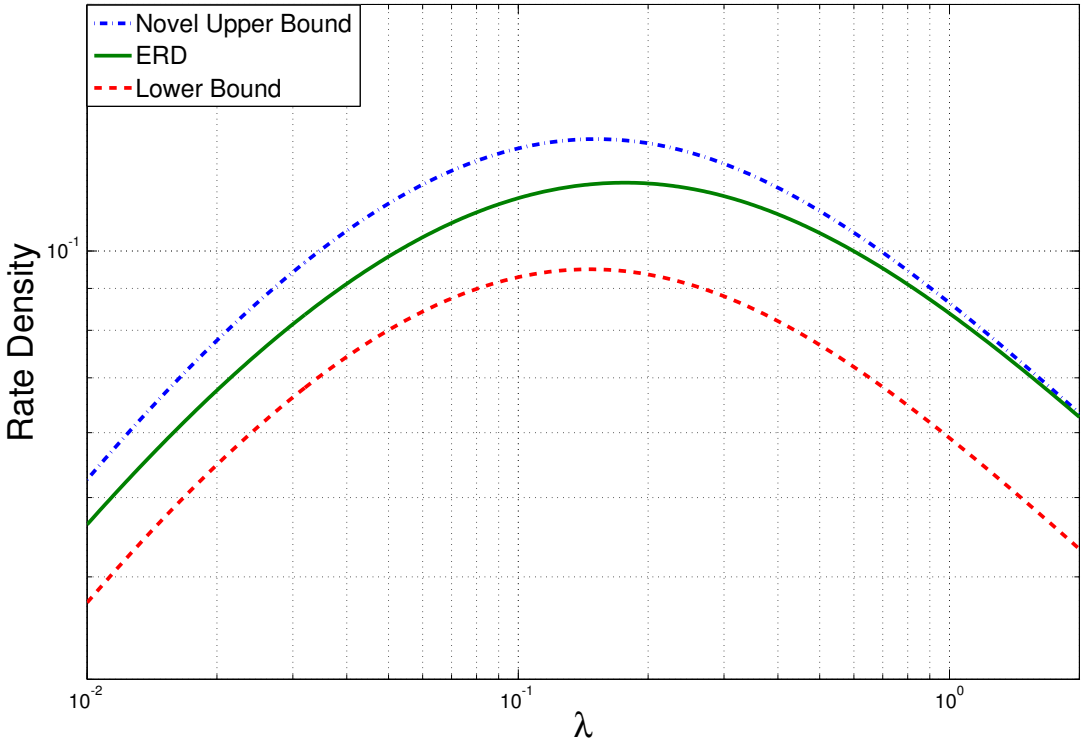

Fig. 1. Rate density as a function of active user density for $\alpha = 3$ and Rayleigh fading channels.

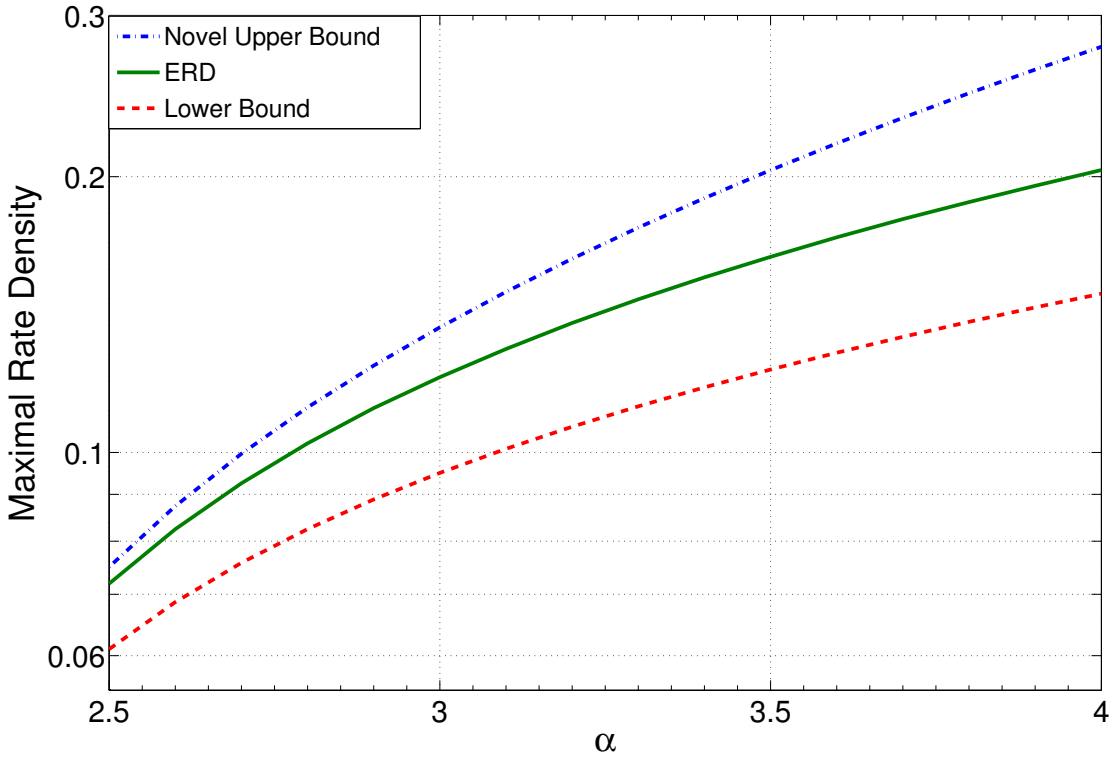

Fig. 2. Maximal rate density as a function of the path loss factor for Rayleigh fading channels.

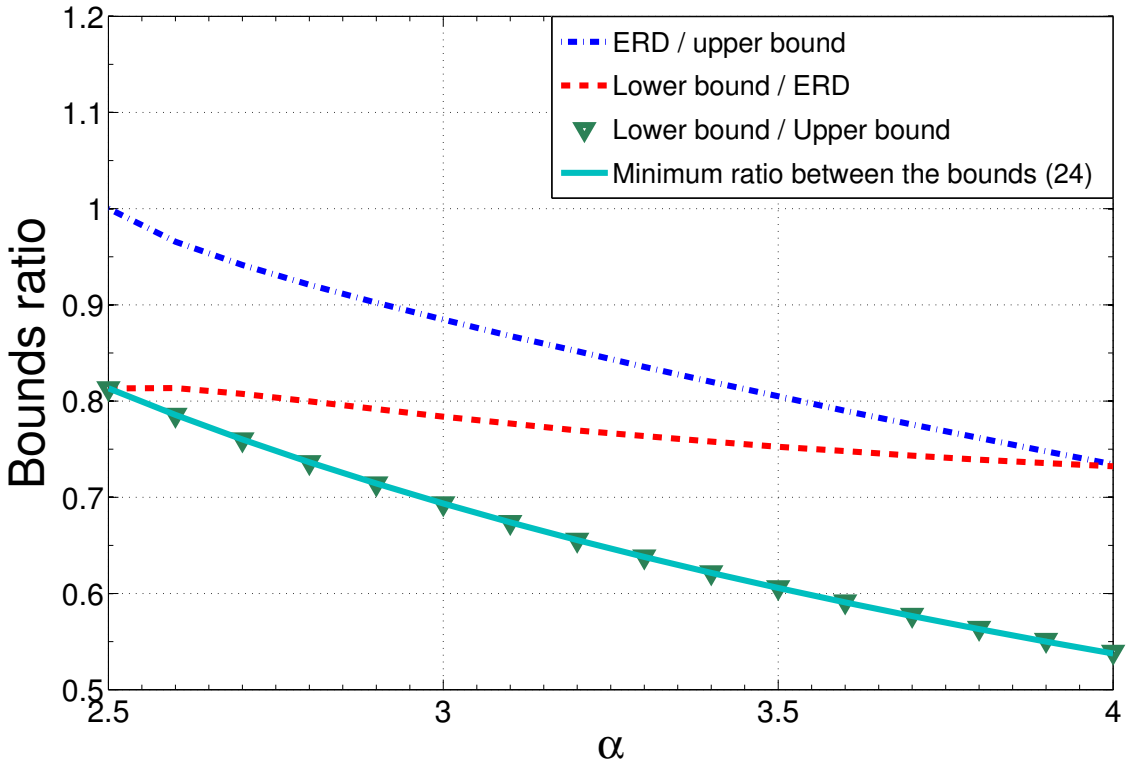

Fig. 3. The ratios between the ERD and the upper bound, the lower bound and the ERD, the lower bound and the upper bound and the minimum bounds' ratio expression (24) as a function of the path loss factor for Rayleigh fading channels.

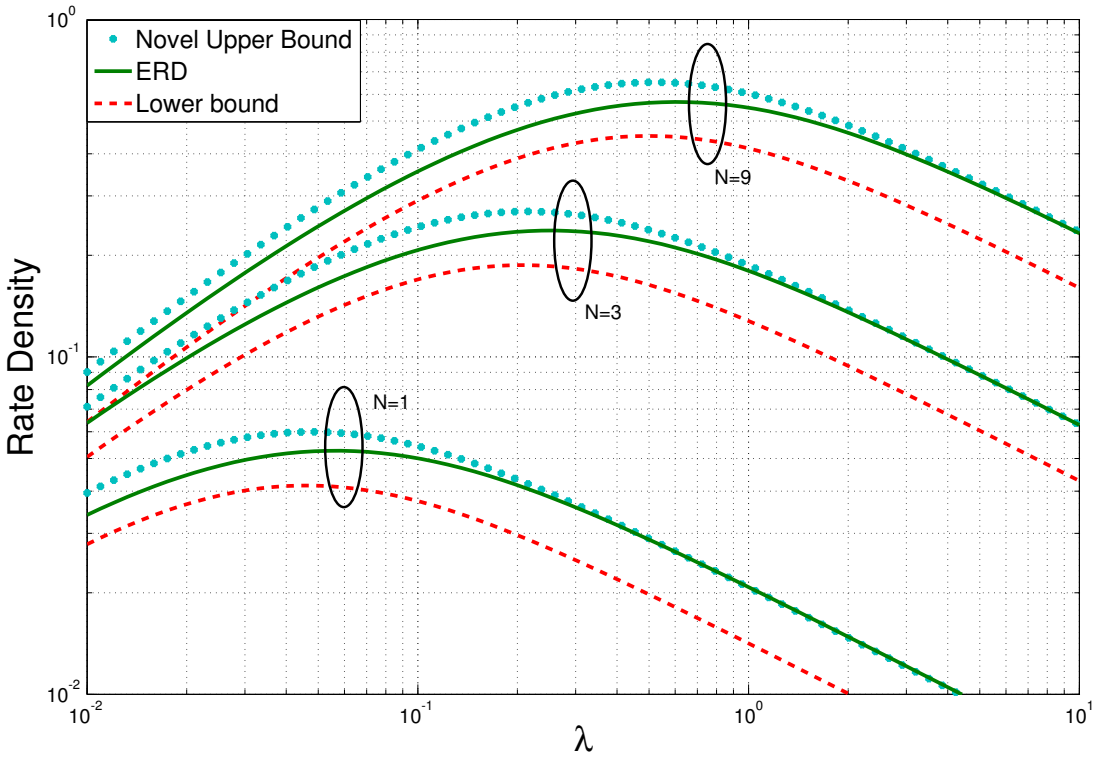

Fig. 4. Rate density as a function of the active user density for transmit beamforming with $M = 1$, $N = 1, 3, 9$, $\alpha = 3$ and Rayleigh fading channels.

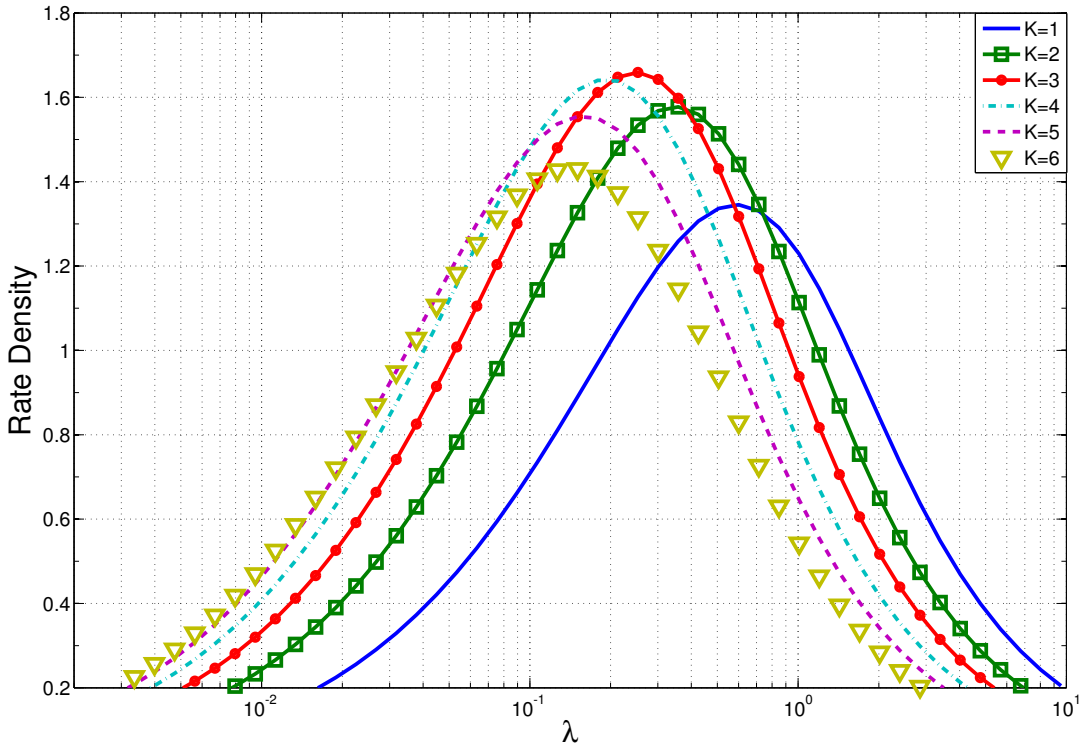

Fig. 5. The upper bound as a function of the active user density for MIMO 6×6, $\alpha = 4$ and $K = 1, 2, 3, 4, 5, 6$ spatial streams.

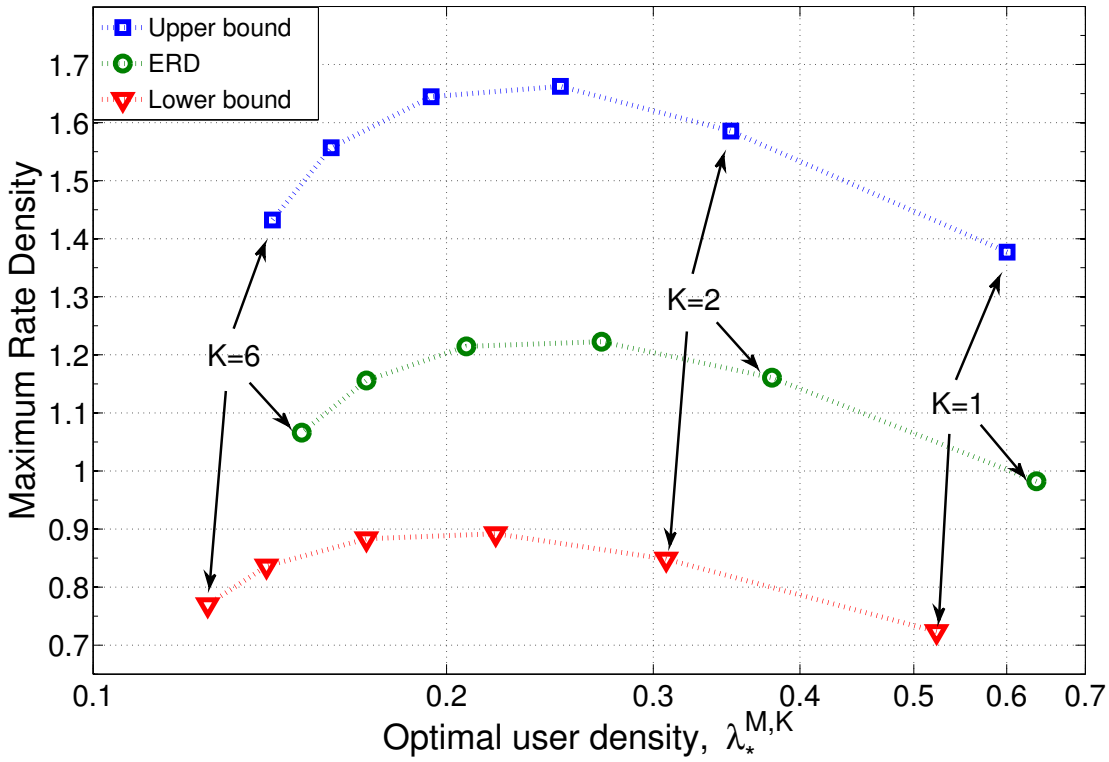

Fig. 6. The maximum rate density of the upper bound, the ERD and the lower bound as a function of the optimal active user density for MIMO 6×6, $\alpha = 4$ and $K = 1, 2, 3, 4, 5, 6$ spatial streams.